Available online at www.sciencedirect.com
SCIENCE DIRECT
Catalysis Today 107–108 (2005) 157–167
CATALYSIS TODAY
www.elsevier.com/locate/cattod

Automotive catalyst deactivation: Case studies

Fatima Maria Zanon Zotin [a,*], Otávio da Fonseca Martins Gomes [b], Cristiano Honório de Oliveira [b], Arnaldo Alcover Neto [b], Mauri José Baldini Cardoso [c]

[a] *Universidade do Estado do Rio de Janeiro, Instituto de Química, Rua São Francisco Xavier, 524 Maracanã, Rio de Janeiro 21550-900, RJ, Brazil*
[b] *Centro de Tecnologia Mineral, CETEM/MCT, Av. Ipê, 900, Cidade Universitária, Rio de Janeiro 21941-590, RJ, Brazil*
[c] *PETROBRAS S.A., R&D Center, Cidade Universitária, Qd. 7, Ilha do Fundao, Rio de Janeiro 21949-900, RJ, Brazil*

Available online 24 August 2005

Abstract

The study of automotive catalyst deactivation is associated with technical, economic and environmental problems. The deactivation phenomenon has different origins that can be divided into three groups: thermal, chemical and mechanical deactivation. In this work, nine commercial catalysts were analyzed, seven of them aged in an engine bench. A study using scanning electron microscopy (SEM) with energy-dispersive X-ray analysis (EDS) at different positions of the monolith allowed the probable reasons for catalyst deactivation to be inferred. Thermal deactivation was a common cause for most of the samples. Other mechanisms such as washcoat losses or abrasion, contamination by sulfur and lubricants, and noble metal sintering were also observed for different samples.

Keywords: Automotive catalyst; Thermal deactivation; Chemical deactivation; Mechanical deactivation; Scanning electron microscopy

1. Introduction

The study of automotive catalyst deactivation is of major relevance because it is associated with environmental aspects as well as economic issues.

According to reports in the literature, the phenomenon of deactivation may have diverse origins [1–15]. It can be divided into three main groups: thermal, chemical and mechanical deactivation [1,2]. Thermal deactivation is related to problems generated by the washcoat sintering process, alloy formation among the compounds, support alterations, interactions among precious metals and other metals, interactions among metals (or metal oxides) and the support, metal volatilization and others. Chemical deactivation involves factors such as catalyst site poisoning (irreversible adsorption or reaction), competitive reversible adsorption of poison precursors and physical/chemical blocking of pores. Mechanical deactivation is related to fractures caused by thermal shock or by impact or attrition.

Thermal deactivation occurs under high temperatures that lead to the sintering of noble metal particles and/or sintering and phase alterations of the compounds that form the washcoat, mainly γ-alumina. This phenomenon is directly related to the composition of the washcoat because many compounds such as La_2O_3, CeO_2 and ZrO_2 give thermal stability to the metals and to the alumina [9,11–14]. According to Arai and Machida [11], pure γ-alumina undergoes consecutive phase changes when submitted to high temperatures. At approximately 1050 °C, γ-alumina turns to δ-alumina, that, at approximately 1150 °C, changes to θ-alumina, which finally turns to α-alumina at 1200 °C. These phase changes cause a significant decrease in the surface area, consequently affecting the catalyst performance.

Additives such as BaO, La_2O_3, CeO_2, ZrO_2 and SiO_2 are used to minimize sintering problems. Cerium and lanthanum are the elements most used for alumina thermal stabilization and their excellent performance is due to the formation of superficial lanthanum and cerium aluminate [11,14]. The

* Corresponding author.
E-mail address: fzotin@uerj.br (F.M. Zanon Zotin).

0920-5861/$ – see front matter © 2005 Elsevier B.V. All rights reserved.
doi:10.1016/j.cattod.2005.07.111

structure of this aluminate layer matches the surface of the transition alumina. In other words, the aluminate and the alumina oxygen layers are similar in terms of anion packing [11], resulting in a strong interaction that inhibits crystal growth and gives higher thermal stability.

Thermal degradation of automotive catalysts begins at temperatures between 800 and 900 °C, or even at lower temperatures, depending on the composition of the catalyst [1]. Experimental data have shown that sintering is strongly dependent on temperature, but is also influenced by the reaction atmosphere, which is more critical in an oxidant medium [15]. Noble metal sintering becomes significant above 600 °C, and the basic sintering mechanism for small metal particles involves diffusion at the surface or, at high temperatures, mobility of larger clusters [1,4,5]. Particle growth by clustering or coalescence is undesirable because it reduces the metallic area, interfering in the electric properties of the metals; depending on the support, these metals can provide electrons or present a lack of them, favoring the adsorption of certain reactants. Metal sintering is also strongly affected by the overall reduction in surface area [5]. The metals used most are platinum, palladium and rhodium. Of these, rhodium is the most sensitive to thermal sintering under the operating conditions for automotive catalysts, decreasing the activity for NO_x reduction. This effect is minimized by using bimetallic catalysts such as Pd-Rh and Pt-Rh [1]. The reaction atmosphere is also an important parameter. Sintering of platinum particles is favored in an oxidant medium. On the other hand, Pd is more active in the oxide form (PdO), but between 600 and 800 °C, the decomposition of PdO to metallic Pd occurs, followed by a decrease in catalytic activity [5]. After the reduction of PdO to Pd^0 at high temperatures, redispersion of the metal with decreasing temperature may be observed. However, an activity hysteresis of up to 100 °C is common. The sintering process after the formation of metallic Pd is more pronounced in inert or oxidant atmospheres [5].

Concerning chemical deactivation, the effect of lubricant oil contaminants on automotive catalyst performance is well known. Contaminants such as phosphorus, zinc and calcium are deposited on the catalyst surface, blocking the active sites. Zinc and calcium remain in the external layer of the catalyst, whereas phosphorus migrates to the washcoat and interacts with cerium oxide and alumina, forming phosphates [7,8].

Another important contaminant is sulfur present in the fuel. Many articles have been published on this topic, and all of them emphasize the complexity of the system formed by the automotive catalyst, its operating conditions and interaction with sulfur compounds [3,5–7,15].

One of the exhaust gas components is SO_2, which is formed when fuel that contains organic sulfur compounds is burned. As it passes through the catalyst, part of this SO_2 may interact with the washcoat components and with steam, in the latter case producing sulfuric acid and presenting an additional problem regarding emissions. Interaction with the washcoat is complex and depends on the temperature and composition of the gas (rich or poor conditions). Under oxidant conditions, SO_2 may interact with the metal and form SO_3 on the surface of this metal. Thus, alumina and CeO_2 may also be sulfated, which consequently interferes in the metal–support interaction. These compounds are adsorbed at low temperatures (up to 300 °C) but they need high temperatures to desorb (above 650 °C). Under reducing conditions (rich phase, low oxygen levels in the medium) part of the adsorbed SO_2 turns to H_2S, another catalyst contaminant due to its strong interaction with metallic surfaces. Poisoning by sulfur is more critical at low temperatures. At high temperatures (1000 °C, for instance), there is no adsorption of these compounds. Most of the SO_3 formed reacts with alumina and CeO_2 and, on a smaller scale, with the metal. When alumina is used as the support, the tolerance to sulfur is greater because it acts as a trap for SO_2 molecules. Therefore, a support that has lower specific surface area or that has undergone phase changes has a lower adsorption capacity for SO_2.

As observed above, catalyst deactivation is related to many factors. Thus, the objective of this work was to identify the main causes of deactivation of commercial automotive catalysts by characterizing used samples by means of scanning electron microscopy (SEM) with attached energy-dispersive X-ray analysis (EDS).

2. Experimental

In this research, a group of commercial automotive catalysts from the same manufacturer was used (Table 1), all of them containing Pd and Ni. These catalysts were aged in an engine bench using a 150 or 300 h test, with the latter condition being considered representative of the aging suffered by a catalyst after 80,000 km [2]. Catalysts C and F underwent more drastic thermal aging (>1100 °C). The tests were not exactly similar for all the catalysts. The aging temperature, cycle time and vehicle speed were varied with the objective of simulating typical situations for engine malfunction. Gasolines with two different sulfur levels (400 and 700 ppm) were used so that chemical deactivation by this element could also be investigated. Fresh catalysts from the same manufacturer's series were also used as reference samples.

The BET surface area of the catalysts was measured using an ASAP 2400 V3.07 analyzer. Analyses were performed on

Table 1
Commercial catalyst samples and respective aging procedures

Catalyst	Aging test	Sulfur (ppm)	Time of aging (h)
A	Yes	700	300
B	Yes	700	300
C	Yes	400	150
D	Yes	400	300
E	Yes	400	300
F	Yes	700	300
G	Yes	700	300
H	No	–	–
I	No	–	–

three areas of the catalysts, inlet, middle and outlet, using catalyst fragments, including the cordierite support. The pore volume of the same sample was also measured. Test samples for SEM analysis were prepared by longitudinal sectioning of each catalyst in four equal parts. One of these parts was inserted in epoxy resin for each catalyst. Then, three slices, approximately 1 cm thick, were sawn perpendicularly to the monolith channels, one in the inlet, one in the center and another in the outlet. Each slice was polished with diamond abrasives up to a grain size of 1 μm and then covered with carbon. This method of preparing the test samples also allows analysis of the radial and axial distribution of contaminants and structural changes. These samples were analyzed in a LEO S440 SEM equipped with a Link ISIS L300 EDS microanalysis system with a SiLi Pentafet detector, ultrathin ATW II window and resolution of 133 eV at 5.9 keV. All the analyses were carried out at an electron acceleration potential of 20 kV. The images were obtained with a backscattered electron detector (BSD) and, eventually, a secondary electron detector (SED) for observing morphological details. The resolution of the EDS analysis was a circle of approximately 1 μm in radius and 1.5–3.5 μm deep, depending on the material density at the analysis point.

X-ray diffraction (XRD) patterns of the catalysts were obtained in a Siemens AXS D5005 instrument using Cu Kα radiation at a scanning rate of 2°/min in the range between 2° and 70°. To minimize the influence of the cordierite support on the diffraction patterns, the surface of the catalysts were grated to collect a sample of the washcoat portion, which was subsequently fixed on adhesive tape and analyzed by diffractometry.

Table 2
Textural properties of fresh and aged catalysts

Catalyst	Surface area (m^2/g)	Microporous surface area (m^2/g)	Pore volume (cm^3/g)
A	4.1	1.8	0.009
B	4.0	1.6	0.009
C	1.1	1.3	0.001
D	7.7	1.3	0.034
E	20.2	0.4	0.065
F	3.5	–	–
G	19.4	1.7	0.067
H	27.4	4.3	0.067
I	34.4	0.1	0.090

3. Results

The nine commercial catalysts studied were designated as A–I, of which the first seven were submitted to the 300 h aging test in an engine bench, except for catalyst C, which was aged for a period of 150 h. Two of them were tested in a bench simulating a poor burn (catalysts F and C), a typical engine malfunction that promotes a high concentration of unburned gasoline in the catalyst. The fresh catalysts were designated as H and I.

Textural properties of the fresh and aged catalysts are shown in Table 2. These values were obtained by averaging the values obtained for the three longitudinal positions to minimize axial differences. These results demonstrate that the catalysts were not microporous, but presented a mesoporous texture with porous diameters between 20 and 200 Å. Comparing the surfaces areas of the aged catalysts, sample C was most affected by the aging procedure, followed by F, A,

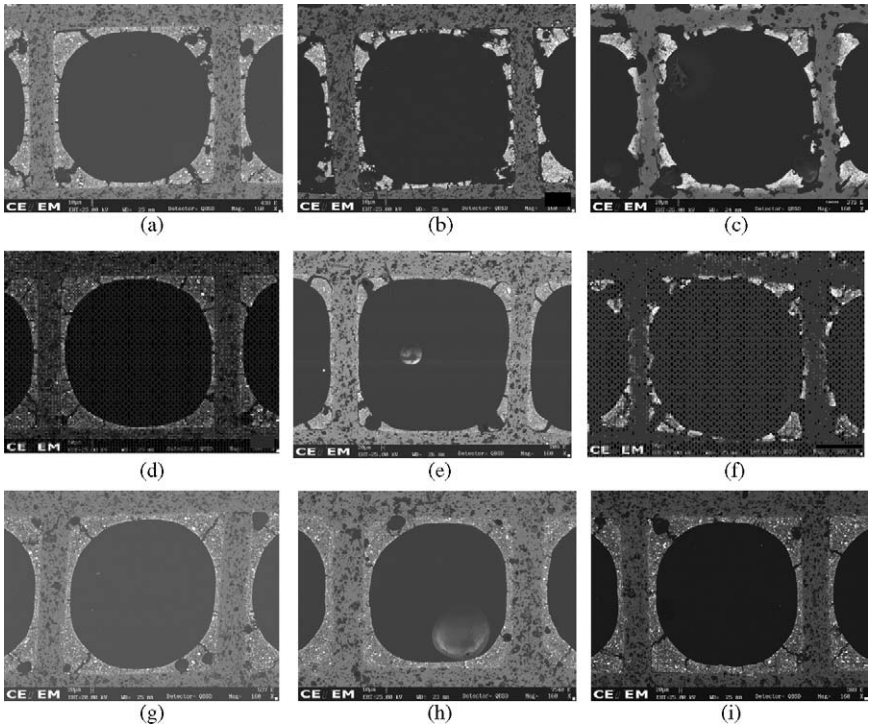

Fig. 1. Front view of channels in the inlet region of the studied catalysts A (a), B (b), C (c), D (d), E (e), F (f), G (g), H (h) and I (i).

B, D, G and E. This sequence was reasonable, considering that the thermal aging was more drastic for catalysts C and F, though catalyst C was aged for only 150 h. Results for the pore volume are in accordance with the surface area values.

SEM images of the catalysts studied are presented in Fig. 1; the images shown are of the inlet section, chosen for being most affected by either physical or chemical deactivation processes. It is evident that catalysts B, C and F showed significant material loss in this region.

Sectional analysis showed that for catalyst B, material loss was more significant in the inlet region, less in the center and almost absent in the outlet (Fig. 2).

In contrast, for samples F and C, damage was greater, reaching the entire central region. This material loss is probably related to the sintering of the active phase (washcoat) observed in these catalysts. Distortion of the cordierite monolith in some positions in catalyst C, and principally in F, was also observed, being stronger in the outlet portion of the monolith. This is compatible with temperatures attaining values higher than 1200–1400 °C (cordierite melting) (Figs. 3 and 4).

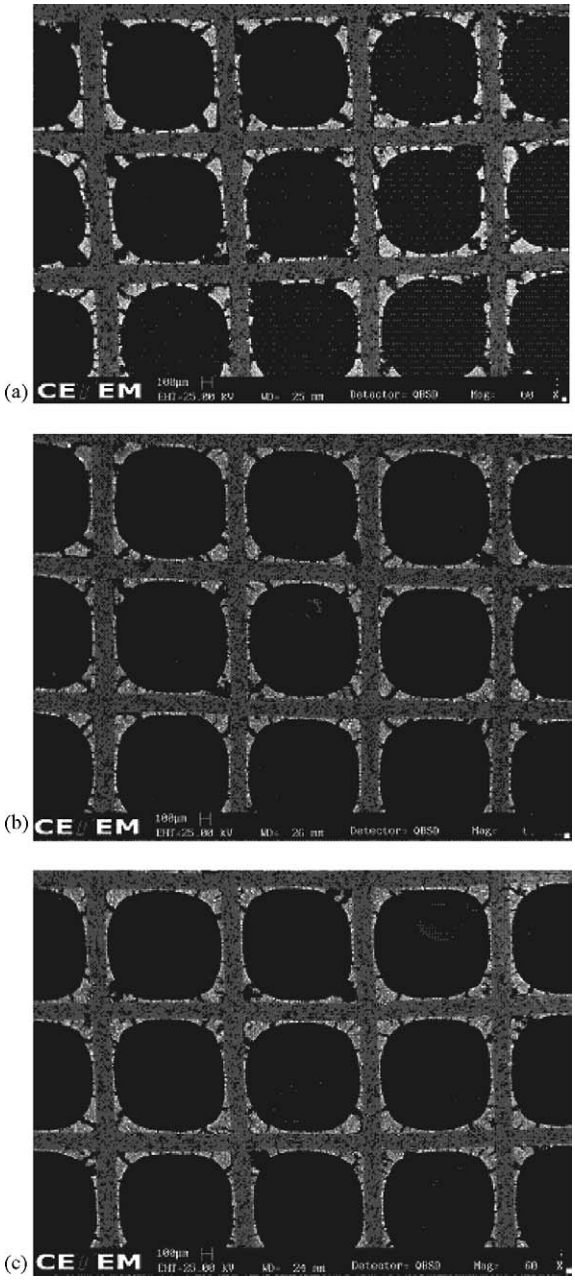

Fig. 2. Front view of the inlet (a), middle (b) and outlet (c) regions of the catalyst B.

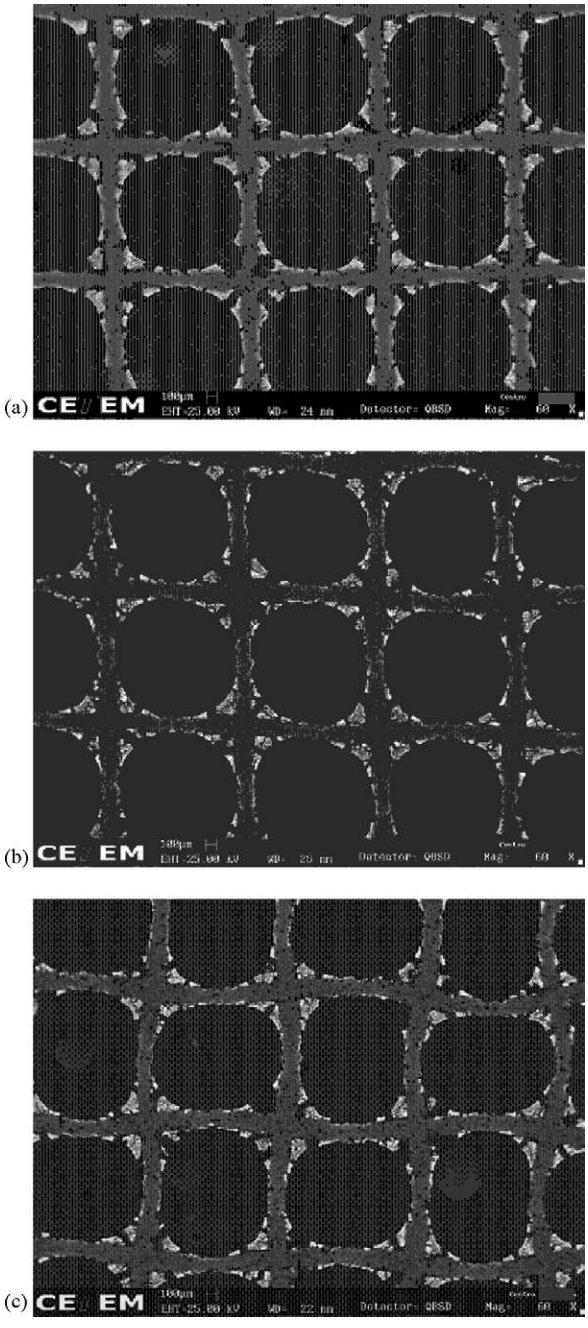

Fig. 3. Front view of the inlet (a), middle (b) and outlet (c) regions of the catalyst C.

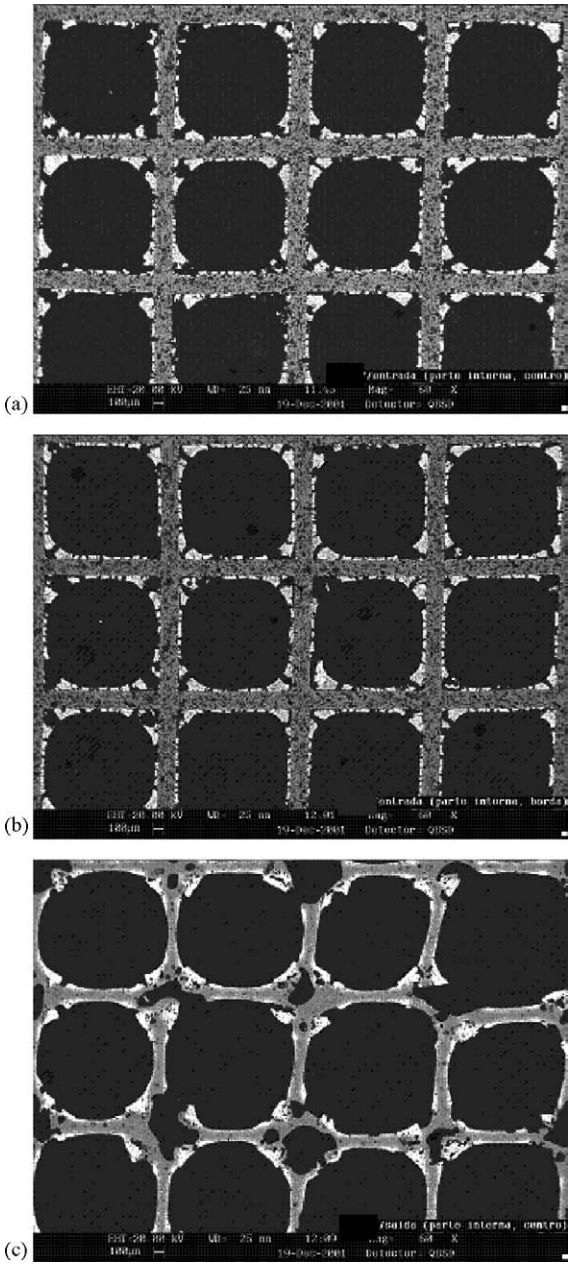

Fig. 4. Front view of the inlet (a), middle (b) and outlet (c) regions of the catalyst F.

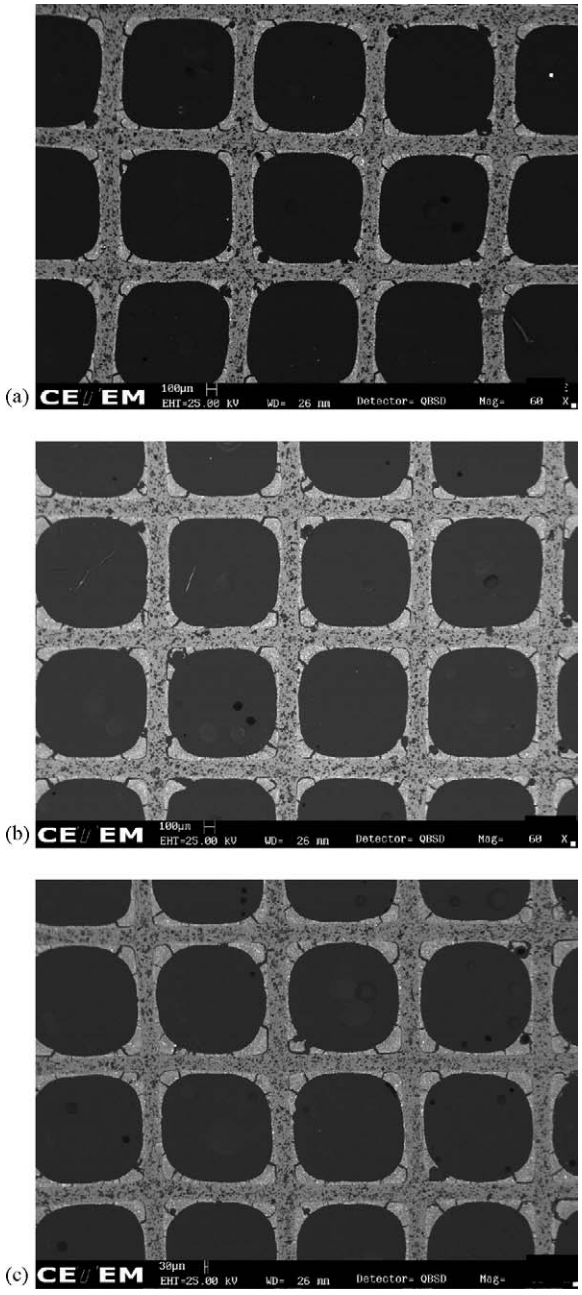

Fig. 5. Front view of the inlet (a), middle (b) and outlet (c) regions of the catalyst E.

The image of catalyst E (Fig. 5) also suggests material loss, not by washcoat loosening, as in the previous cases, but by abrasion. The quantity of catalyst material on the wall of a channel (thickness of the washcoat layer) is clearly smaller than that observed in the fresh catalysts (Fig. 1, catalysts H and I; Fig. 6, catalyst I). These losses were greater in the inlet, whereas at the outlet the washcoat remained intact. Therefore, mechanical deactivation seems to be predominant.

In this first analysis, catalysts A, D and G appeared to be intact without washcoat sintering or material loss, similar to fresh catalysts H and I.

Local chemical compositions of the used catalysts were determined by EDS. Images and EDS spectra for catalysts B and F are shown in Fig. 7. Catalyst B, aged in a 300 h test, showed washcoat loss in the inlet region (Figs. 1 and 2) and, according to the EDS results (Fig. 7a), contamination by sulfur associated with nickel and palladium. Palladium, on the other hand, was observed in large aggregates, as can be seen in Fig. 7b. This image is interesting because it shows a large Pd particle (≅1 μm) associated with Ni, surrounded by a region rich in sulfur and nickel, confirming that the noble metal, sulfur and nickel are in close interaction in these catalysts.

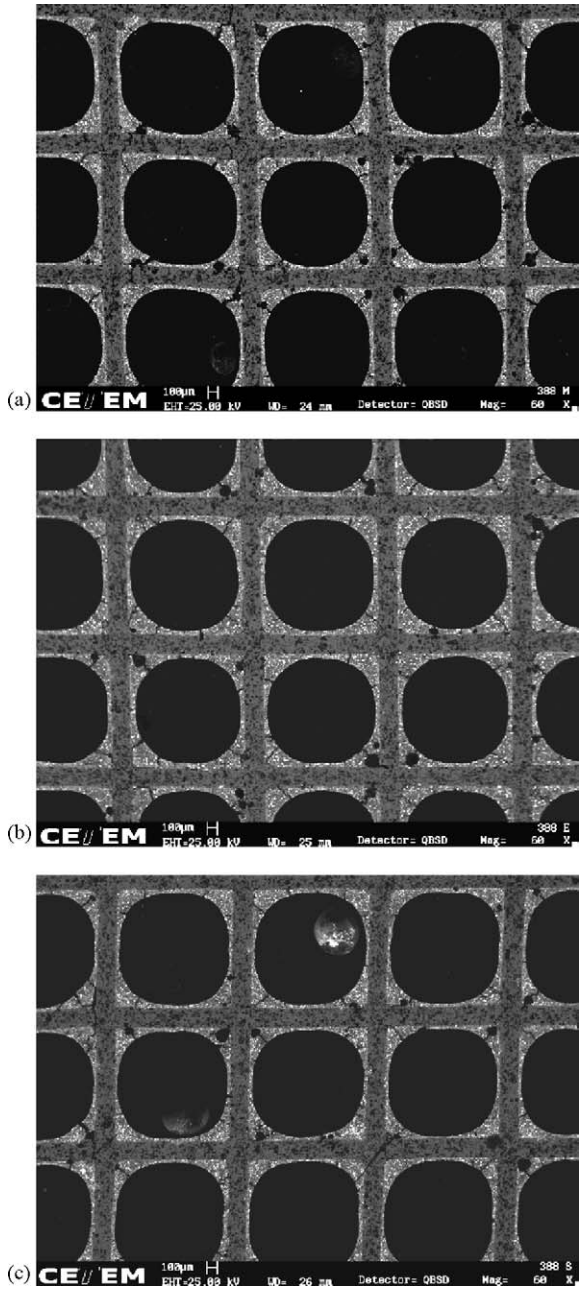

Fig. 6. Front view of the inlet (a), middle (b) and outlet (c) regions of the catalyst I.

For catalyst F submitted to the 300 h test, the SEM results show that there was thermal deactivation together with catalytic material loss (Figs. 1 and 4) during the aging procedure. Moreover, as indicated in Fig. 7c, the presence of chemical contaminants was also observed, especially phosphorous and calcium, both lubricant oil additives.

Fig. 8 shows details for catalysts D, E and A. Catalyst D retained its integrity after this procedure, without evidence of material loss. However, more detailed analysis of its surface indicated the presence of large palladium particles. No signs of chemical contamination were observed (Fig. 8a).

For catalyst E, some abrasion was noted, mainly in the inlet region, as indicated in Figs. 1 and 5. Fig. 8b shows sulfur contamination on this sample, always associated with nickel. Palladium remained dispersed.

Catalyst A did not suffer significant washcoat losses, as evident from Fig. 1. On the other hand, Fig. 8c shows the presence of large Pd particles.

For catalyst C, damage due to thermal aging was very significant, as can be observed in Figs. 1C and 3. Fig. 9 shows two slides for catalyst C at higher magnification and with elemental analysis; the first one (Fig. 9a) shows an image obtained at the catalyst inlet, where it was impossible to identify the different particles constituting the washcoat, confirming the severe thermal treatment undergone by this catalyst. The second slide (Fig. 9b), of the outlet of the same catalyst, shows a sample with a more preserved textural appearance, indicating that the outlet position was less affected by the high temperatures. No evidence of chemical contamination was indicated by the chemical analysis. Catalyst G presented a similar aspect to the fresh catalysts (Fig. 1g), as can be observed in Fig. 9c, in which there is no evidence of thermal damage. This could be an indication that the temperature used in thermal aging was lower than in the previous case. Sulfur was present on the surface of catalyst D.

It is interesting to point out the presence of many large palladium particles (catalysts A, B, D). Metal phase sintering begins at approximately 600 °C [1]. Besides the significant reduction in metallic surface area and the consequent loss of activity, temperatures above 800 °C lead to the reduction of PdO, the most active form of Pd, to Pd^0, leading to an additional decrease in catalytic activity. Thus, thermal effects on palladium are undesirable for two reasons.

Problems related to chemical contamination were also identified. The presence of sulfur on the catalyst surface was clear and is a consequence of the high level of this element in the gasoline used for catalyst aging. A summary of the possible deactivation causes in the catalysts studied is presented in Table 3.

The effect of thermal deactivation can also be observed from the XRD results. Fig. 10 shows diffraction patterns for catalysts C and I. XRD spectral analysis of fresh or exhausted commercial automotive catalysts is complex due to the many components and contaminants involved. XRD data for the fresh catalyst (Fig. 10a) indicate the presence of cerium oxide, nickel oxide and cordierite (impurity as a result of washcoat grating). Although Al was observed by EDS in the washcoat of fresh samples, the characteristic diffraction peaks of Al_2O_3 were not observed, probably due to its low crystallinity. Thermal aging generally promotes an increase in sample crystallinity and it is possible to identify the α-alumina phase in catalyst C, for example (Fig. 10b).

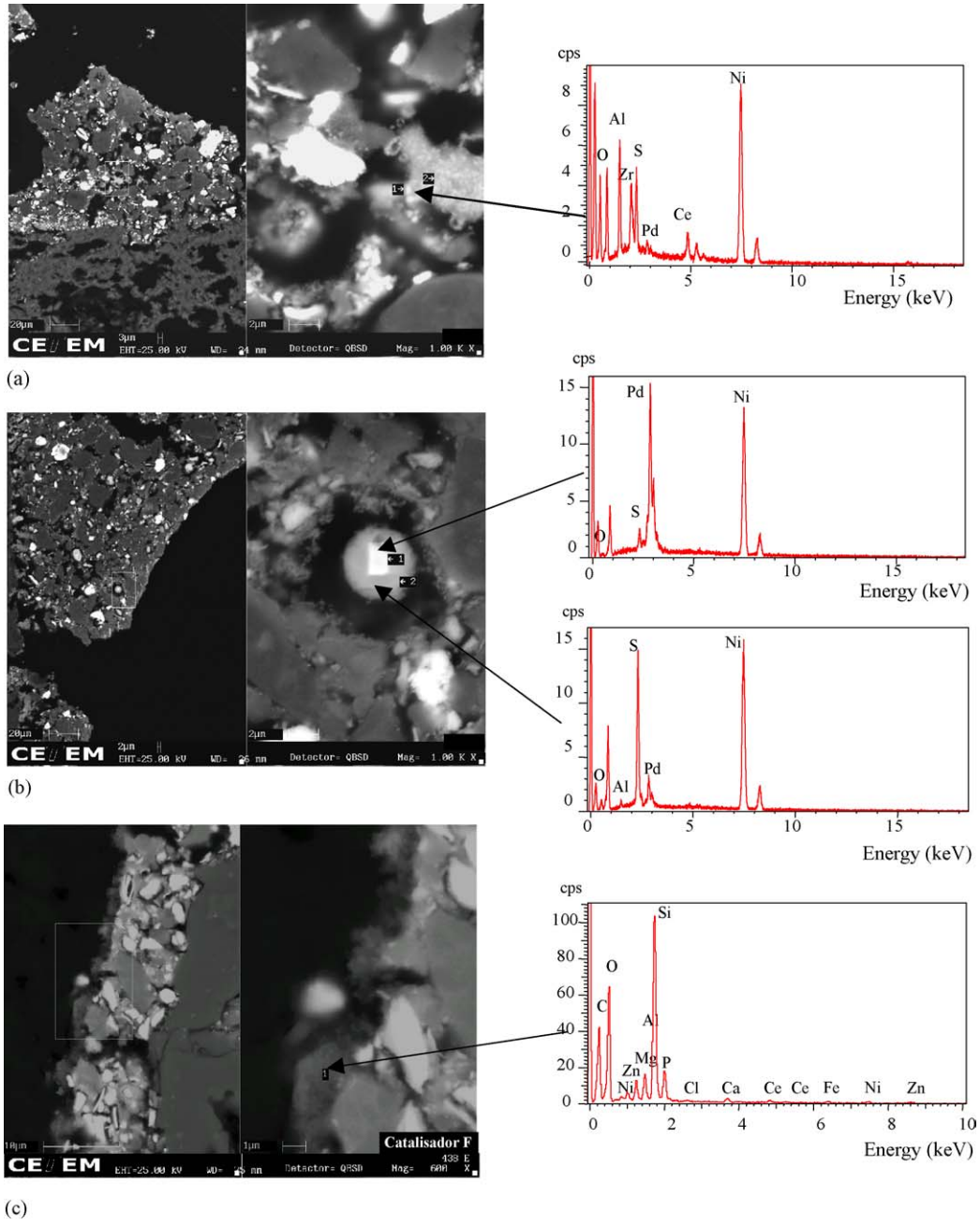

Fig. 7. Details of catalyst B (a and b), catalyst F (c).

As observed, most of the catalysts showed thermal deactivation, even excluding the catalysts aged under engine malfunction (C and F). The most common effect was palladium sintering (catalysts A, B and D), and under high temperatures, washcoat sintering and damage of the cordierite structure. Apparently, high temperatures were also responsible for loss of the sintered washcoat.

It was observed, as expected, that palladium and nickel have high affinity with sulfur. On one hand, palladium–sulfur interaction will decrease the number of sites available for the conversion of pollutants in the exhaust gas. Nickel–sulfur interaction, on the other hand, is expected because the function of this metal is to remove sulfur from the reaction medium, minimizing its interaction with palladium and H_2S emissions to the atmosphere.

Sulfur contamination was observed in most of the samples, usually associated with Ni and Pd particles. However, there was no clear correlation with the sulfur content of the gasoline, as samples submitted to 400 or 700 ppm sulfur displayed sulfur associated with the washcoat.

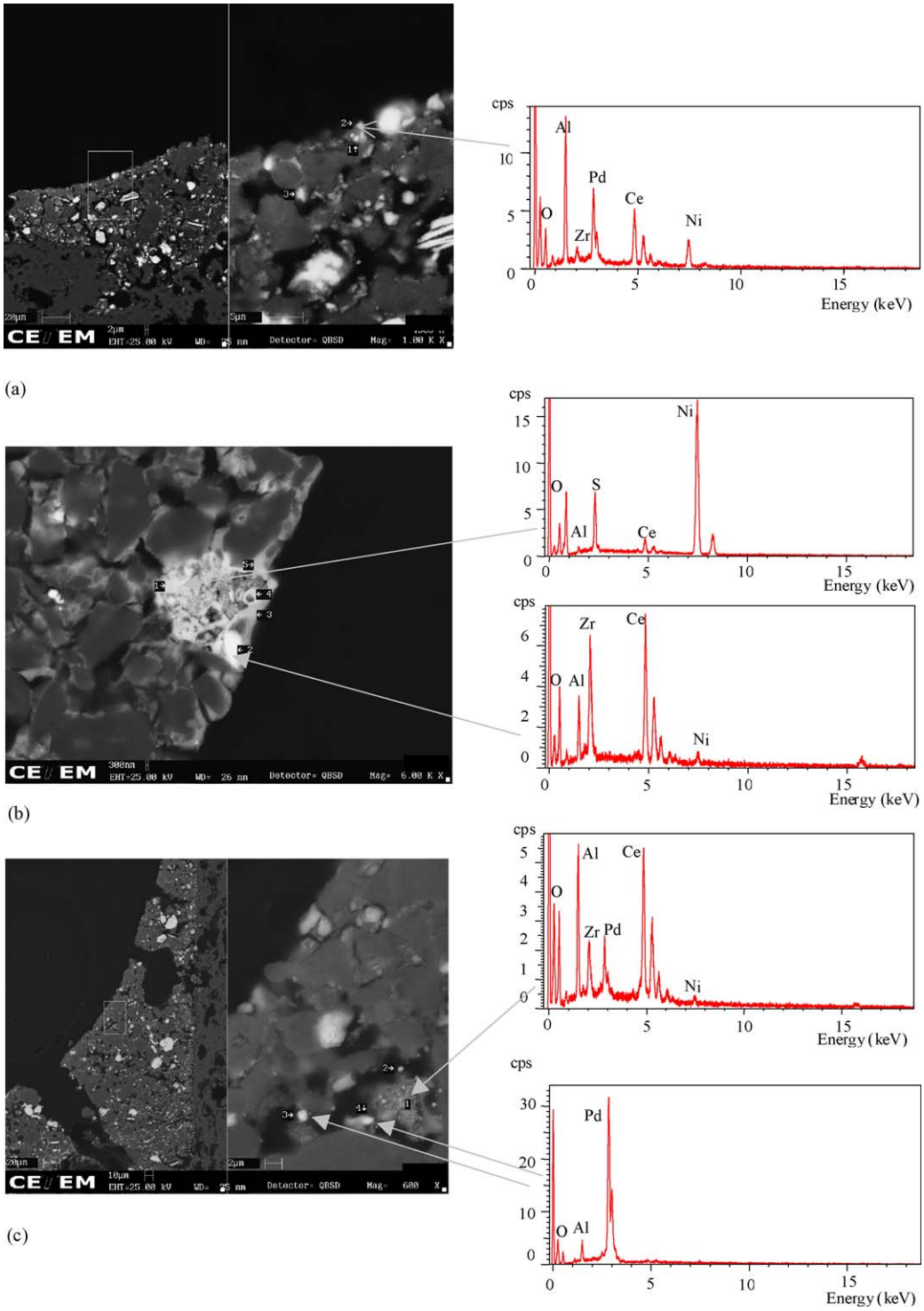

Fig. 8. Details of catalyst D (a), catalyst E (b) and catalyst A (c).

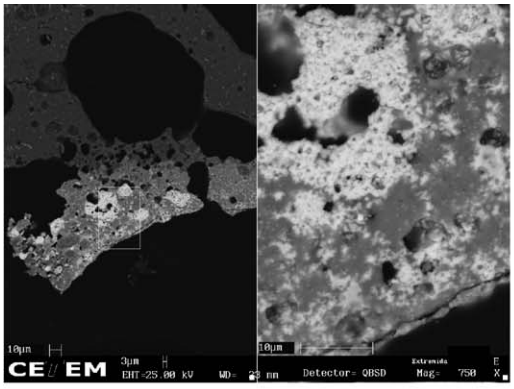

(a)

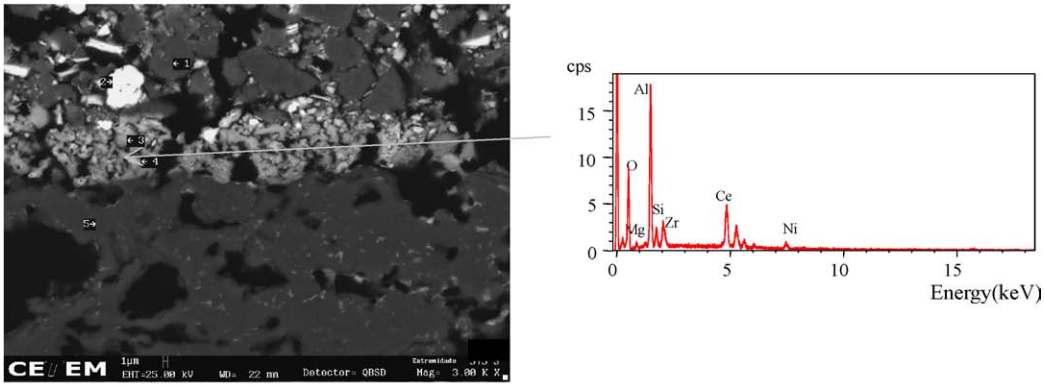

(b)

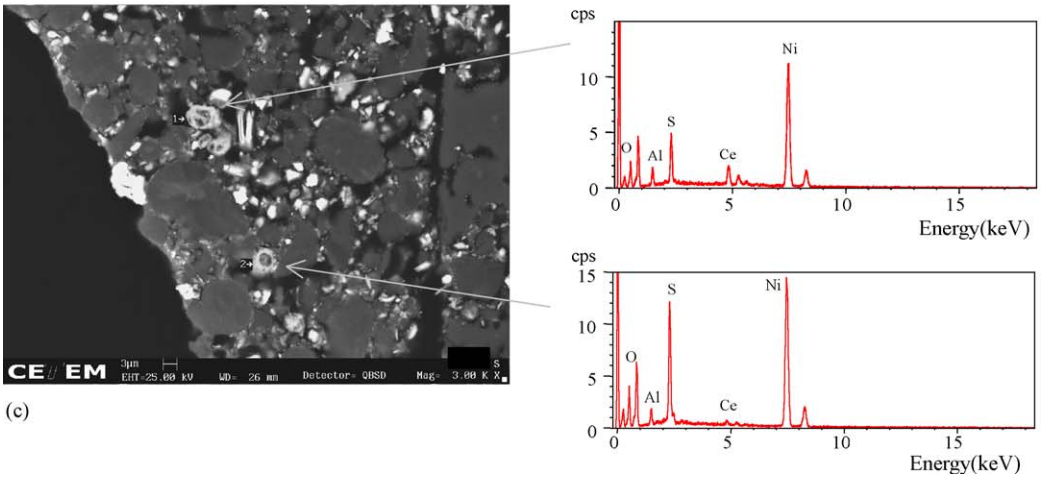

(c)

Fig. 9. Details of catalysts C and G: (a) catalyst C (inlet), (b) catalyst C (outlet) and (c) catalysts G.

Table 3
Deactivation causes identified

Catalyst	Physical aspects	Contaminants (from EDS)
A	No damage; without washcoat sintering aspects or loss material; large palladium particles	Contamination by sulfur
B	Loss material in inlet region; large palladium particles	Contamination by sulfur (interaction with nickel and palladium)
C	Sintered; important loss material	Difficulty to identify the contaminants (high sintering)
D	No damage; without washcoat sintering aspects or loss material; large palladium particles	No indication of chemical contamination
E	Material loss by abrasion (mainly in inlet region); Pd kept disperse	Contamination by sulfur (interaction with nickel)
F	Sintered; important loss material	Contamination by P and Zn (additives of lubricant oil)
G	No damage; without washcoat sintering aspects or loss material; Pd kept disperse	Contamination by sulfur (interaction with nickel)

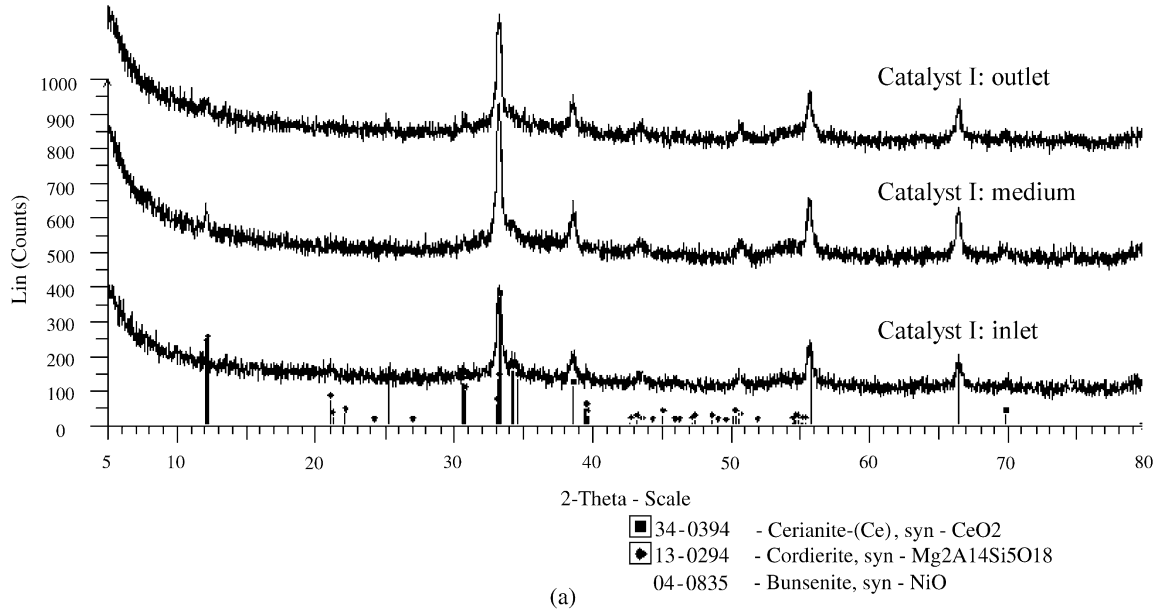

Fig. 10. XRD data: (a) catalyst I and (b) catalyst C ((*) symbol corresponds to diffraction peaks which can be associated with α-Al_2O_3).

4. Conclusions

The group of commercial automotive catalysts analyzed allowed us to characterize the main causes of automotive catalyst deactivation, such as noble metal sintering (A, B and D), washcoat loss due to thermal effects (B, C and F), washcoat loss by abrasion (E), sulfur contamination (A, B, E and G), lubricant oil contamination (F), and sintering (C and F). The clear observation of sintering problems and chemical contamination by sulfur and lubricant oil was possible by simulating situations of engine malfunction and by using gasoline with high sulfur levels, respectively. It was also clear that catalyst deactivation does not necessarily occur for one single reason, but in most cases is due to a combination of thermal, chemical and sometimes, mechanical effects.

Acknowledgement

The authors gratefully acknowledge financial support from PETROBRAS S.A.

References

[1] U. Lassi, Deactivation Correlations of Pd/Rh Three-way Catalysts Designed for Euro IV Emission Limits, Oulu University Press, Oulu, 2003.
[2] G.C. Kultsakis, A.M. Stamatelos, Prog. Energy Combust. Sci. 23 (1997) 1.
[3] T. Luo, J.M. Vohs, R.J. Gorte, J. Catal. 210 (2002) 397.
[4] U. Lassi, R. Polvinen, S. Suhonen, K. Kallinen, A. Savimäki, M. Härkönen, M. Valden, R. Keiski, Appl. Catal. A: Gen. 263 (2004) 241.
[5] A.K. Neyestanaki, F. Klingstedt, T. Salmi, D.Y. Murzin, Fuel 83 (2004) 395.
[6] H.N. Rabinowitz, S.J. Tauster, R.M. Heck, Appl. Catal. A: Gen. 212 (2001) 215.
[7] F.M.Z. Zotin, F.B. Noronha, L.G. Appel, In: J. Blanco, P. Avila (Org.). Catalizadores y Adsorbentes para la Protección Ambiental la Región Iberoamericana, CYTED—Subprograma V. 2a. ed. Madrid, vol. 1, 2001, pp. 127–132.
[8] A. Alcover Neto, F.M.Z. Zotin, R. Neumann, R.L.C. dos Santos, G. Bortolon, S. Fontes, L. Appel, in: Proceedings of Nineth Congresso Brasileiro de Catálise, Águas de Lindóia, vol. 2, 1997, p. 464.
[9] F.M.Z. Zotin, M.J.B. Cardoso, G.F. Bortolon, A. Alcover Neto, in: Proceedings of the 18th Simposio Iberoamericano de Catálisis, Potomar, Venezuela, 2002.
[10] G. Smedler, S. Lundgren, A. Romare, G. Wirmark, SAE 910173 (1991) 11.
[11] H. Arai, M. Machida, Appl. Catal. A: Gen. 138 (1996) 161.
[12] J.R. González-Velasco, J.A. Botas, R. Ferret, M.P. González-Marcos, J.L. Marc, M.A. Gutiérrez-Ortiz, Catal. Today 59 (2000) 395.
[13] X. Wu, L. Xu, D. Weng, Appl. Surf. Sci. 221 (2004) 375.
[14] A. Piras, A. Trovarelli, G. Dolcetti, Appl. Catal. B: Environ. 28 (2000) 77.
[15] D.D. Beck, J.W. Sommers, C.L. DiMaggio, Appl. Catal. B: Environ. 11 (1997) 273.